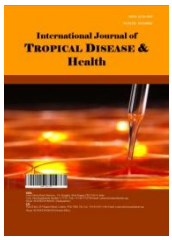

International Journal of TROPICAL DISEASE & Health

43(15): 1-16, 2022; Article no.IJTDH.89422
ISSN: 2278–1005, NLM ID: 101632866

‘Spread’ of Artemisinin Resistance in Myanmar Revisited

Eric P. M. Grist [a*]

[a] *College of Engineering, Mathematics and Physical Sciences, University of Exeter, Exeter, UK.*

Author’s contribution

The sole author designed, analysed, interpreted and prepared the manuscript.

Article Information

DOI: 10.9734/IJTDH/2022/v43i1530643

Open Peer Review History:
This journal follows the Advanced Open Peer Review policy. Identity of the Reviewers, Editor(s) and additional Reviewers, peer review comments, different versions of the manuscript, comments of the editors, etc are available here: https://www.sdiarticle5.com/review-history/89422

Original Research Article

Received 15 May 2022
Accepted 22 July 2022
Published 01 August 2022

ABSTRACT

Geostatistical models have been widely used to represent disease prevalence in spatial disease mapping. More recently, these models have been employed to estimate geographic ‘spread’ of artemisinin resistance (AR) in South East Asia from genetic mutations identified in the K13 gene of the malaria *Plasmodium falciparum* parasite. Here, I revisit the question of ‘spread’ of AR as represented by resistant *plasmodium falciparum* in Myanmar, when re-evaluated from K13 mutant alleles data published by Tun et al. [1]. The new analysis gives a broader perspective by incorporating information published by the World Health Organization (WHO) in 2015 and subsequently in 2018 of the K13 mutant alleles confirmed to confer or to be associated with artemisinin resistance. This provides insights which hitherto have not been described and reveals the disparity between the estimation of ‘spread’ of AR by Tun et al. [1] and that of AR prevalence based on metrics which are supported by published WHO data.

Keywords: K13; genetic markers; overestimation; prevalence; malaria; antimalarial drug resistance.

1. INTRODUCTION

Malaria is caused by a microscopic *Plasmodium* parasite conveyed into humans by some of the mosquito species in the *Anopheles* genus. Antimalarial drugs have long been developed to combat the disease, but their effectiveness has been shown to typically decrease with time as antimalarial drug resistance evolves in certain regional populations (e.g. [2]). More recently,

**Corresponding author: Email: epmgrist@gmail.com*

there has been an emphasis on geostatistical maps to describe the regional status of antimalarial drug resistance in epidemiological mapping studies [3-5,1,6]. Such mappings attempt to depict the prevalence of antimalarial drug resistance in a geographical region using geostatistical models parameterized with data taken from infected persons, but the data are typically limited in sample size and spatial distribution. Their accuracy is dependent also upon the choice of metric used to denote antimalarial drug resistance as well as what constitutes statistical significance for the gathered data. For relatively recent antimalarial drugs such as artemisinin, the uncertainty surrounding all these factors remains largely unresolved. This leaves assessments of antimalarial drug resistance and interpretation of its 'spread' open to overestimation and sensationalization as a scaremongering tactic [7,8,1], which could arguably lead to a conflict of interest in disease mitigation strategies.

The efficacy of an antimalarial drug is typically evaluated by recording the time taken for an arbitrary fixed percentage (usually 50%) of malaria parasites to be cleared from an infected person after administering the drug. If the parasite clearance time, when measured over a large number of infected individuals in a given geographical region is statistically slower than a specific, yet arbitrary average, then antimalarial resistance to the drug in use is deemed to be present in the region. Although the assumption of delayed parasite clearance times equating with the presence of artemisinin resistant *Plasmodium falciparum* parasites and hence artemisinin resistance (AR) is generally accepted, this has been questioned by some leading authors [9,10]. In line with Tun et al. [1] however, the assumption is accepted as axiomatic for the purposes of this paper.

In the case of artemisinin, concerns of artemisinin-resistant *Plasmodium falciparum* spreading across parts of South-East Asia and in particular Myanmar, have been loudly broadcast [1]. The thesis is assisted by the discovery of a genetic association between specific mutations of the *Kelch13* (K13) gene in the *Plasmodium* parasites with longer malarial parasite clearance times. But it is also important to recognise that parasite clearance delay times vary both with different K13 codon mutations and sampling location [11]. For example, the artemisinin resistance (AR) 'effect' of codon F446I has been measured as mild in northern Myanmar where this mutation predominates [1,12]. In short, the precise causal reasons for the genetic associations and variations in their effect on artemisinin resistance still remain unknown [13,14]. Nevertheless, identification of specific mutant alleles which confer resistance to artemisinin has been the subject of much ongoing research since the discovery was published by Ariey et al. [5].

In 2015, the World Health Organisation (WHO) published a list of K13 mutant allele codon numbers, which at the time were either *confirmed to confer* AR or to be *candidates associated with* AR [15]. This was updated to reflect the current knowledge in a later published list [16]. Such definitive genetic marker information provides a statistical handle, which enables AR to be more rapidly estimated through inference from blood samples taken from infected persons. It is the association of AR resistant *Plasmodium falciparum* with these K13 gene mutations, when observed in spatial locations where infected persons are present, that provides the marker tool for mapping estimated AR prevalence on a geographical basis.

In Tun et al. [1] however, the set of *all* mutant alleles with a codon number greater than 440 (henceforth referred to as the g440 metric) collected in their sampling, was assumed to confer AR. Surprisingly, no supporting scientific data were provided for this assumption and it appears to have been an arbitrary choice based only on codons located in the propeller region of the K13 protein. The g440 metric, was then employed in geostatistical models to generate maps of the estimated 'spread' of artemisinin resistant plasmodium from K13 gene mutations identified in blood sample data obtained at sites across Myanmar. Again, neither the robustness nor the importance of the underlying assumptions made (that all the mutant alleles greater than codon 440 confer AR) was addressed in producing the maps in question. From a scientific standpoint, all these factors are crucial, given that not all these codons necessarily confer AR and that many others, such as A578S, are known to *not* confer AR [17,12,18]. Fairhurst [19] for example, provided a list of mutant alleles known to confer AR, which included only 5 of the mutant alleles employed in the g440 metric of Tun et al.[1].

This raises the important, but unanswered question, of how the choice of g440 metric may have influenced the inference and geostatistical

mapping of estimated 'spread' of AR in Myanmar made by Tun et al. [1]. The purpose of this paper, is therefore, to determine how the choice of metric for K13 mutant allele codons conferring AR from the K13 genetic marker data as published by Tun et al. [1] in Myanmar:

I. influenced the estimation of AR prevalence,
II. compares with estimates based on K13 mutant alleles codons that have been recognised as conferring AR by the WHO.

2. MATERIALS AND METHODS

2.1 Sample Sizes

A first avenue into the strength of the statistical inference possible from the Tun et al. [1] data, is provided by examining the sample sizes at each of the sampled sites. Fig. 1 shows a plot of the sample size distribution when viewed across all samples taken from all the study sites.

This plot immediately reveals the sparsity of larger samples obtained at any specific location and that the vast majority (28, greater than 50%) of the samples were obtained from site samples of less than 5 individuals. The spatial extent of the corresponding information supporting any thesis of 'spread' of AR is thus severely limited. In Tun et al. [1], this limitation is concealed by appealing to plots of local prevalence based on agglomerated data shown only for the local administrative regions (in their Fig. 3).

2.2 Choice of AR Metric

In Table 1, four different AR metrics named Metric 1 to Metric 4 are defined in terms of the K13 mutant alleles of the codon numbers implicated in AR based on the official lists of 2015 and 2018 published by the WHO [15,16].

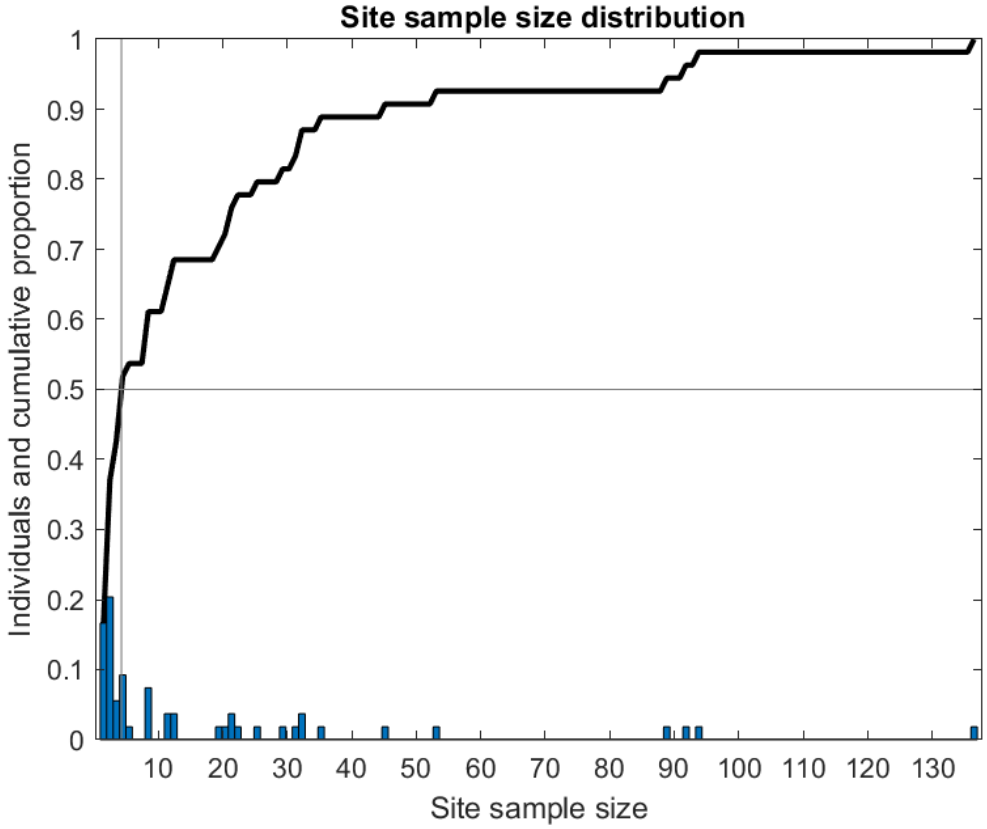

Fig. 1. Site sample sizes of the Tun et al. [1] data. The blue bars show relative frequencies of site sample sizes as a proportion of the total samples collected (*n*=940) with the cumulative proportion superimposed (solid black line). The 50% median percentile (vertical thin line) demonstrates that the majority (28) of the 54 sites sampled had fewer than 5 individuals.

Table 1. K13 mutant allele codons either *confirmed to confer* artemisinin resistance *(*AR) or identified as *candidates to confer* AR by the WHO in the official lists of WHO [15] and WHO [16]. Those shown in bold type were included in the g440 metric of mutant allele codons used to estimate AR 'spread' in Myanmar, as presented by Tun et al. [1]. All codons are listed in full notation (with prefix and suffix letters) in the bottom panel. Those codons employed in Metrics 1 to 4, as defined in this paper to estimate AR prevalence in Myanmar, are listed in the adjacent 4 separate columns.

WHO 2015		Myanmar		WHO 2018		Myanmar	
Confirmed	**Candidate**	**Metric 1**	**Metric 2**	**Confirmed**	**Candidate**	**Metric 3**	**Metric 4**
n=4	*n=9*	*n=1*	*n=8*	*n=9*	*n=11*	*n=5*	*n=14*
493	**441**	**580**	**441**	**446**	**441**	**446**	**441**
539	**446**		**446**	**458**	**449**	**458**	**446**
543	**449**		**449**	**476**	**469**	**476**	**449**
580	*553*		**458**	*493*	**481**	**561**	**458**
	458		**561**	*539*	**527**	**580**	**469**
	561		**574**	*543*	**537**		**476**
	568		**580**	*553*	**538**		**481**
	574		**675**	**561**	*568*		**527**
	675			**580**	**574**		**537**
					673		**538**
					675		**561**
							574
							580
							675

P441L , F446I , G449A , N458Y , C469F , M476I, A481V , Y493H , P527H , N537I , G538V , R539T, I543T , P553L, R561H , V568G , P574L , C580Y , F673I , A675V

These codons fall into two categories within each listed year, respectively defined as either *confirmed to confer* AR, or *candidates to confer* AR at the time of the WHO publications in 2015 and 2018. These findings, therefore, provide 4 logical options for defining an AR metric in terms of codon subgroups:

Metric 1. *Confirmed codons* to confer AR in 2015.
Metric 2. *Confirmed and candidate* codons to confer AR in 2015.
Metric 3. *Confirmed codons* to confer AR in 2018.
Metric 4. *Confirmed and candidate* codons to confer AR in 2018.

These metrics provide a straightforward scientific basis for assessing the estimation of AR prevalence by incorporating official information on K13 mutant alleles codons as published by the WHO in 2015 and in 2018. Metric 1 and Metric 2 respectively correspond to the best-case and worst-case scenarios based on the WHO [15] list. Metric 1 represents the minimum number of codons at 2015 confirmed to confer AR, while Metric 2 represents the potential perceived maximum number of codons that could confer AR. Metric 3 and Metric 4 respectively correspond to parallel definitions as at 2018 based on the WHO [16] list.

Metric 1 consists of the sole codon C580Y, which was the only codon in the Tun et al. [1] data confirmed to confer AR at 2015 by the WHO. A comparison of the codons listed for Metric 2 (8 in total), with those listed for Metric 3 (5 in total), importantly shows that three of the Metric 2 candidate 2015 codons (P441L, P574L, A675V) were still candidates and were not subsequently confirmed to confer AR in 2018. One other WHO [15] candidate, codon *V568G*, and not found in the Myanmar data, also remained a candidate in the WHO [16] list. If this process of incomplete progression (from candidate to confirmed data) continues to the next updated WHO list, yet to be published, it will likely imply that Metric 4 with inclusion of all perceived candidate codons, also gives an *overestimation* of the AR prevalence in Myanmar.

Metric 3 therefore provides a current benchmark as the minimum subset of 5 mutant allele codons found by Tun et al. [1] currently confirmed to confer AR by the WHO. Metric 4 gives an upper bound on Metric 3 as a maximal subset (14 in total) to confer AR as currently reported on the assumption that the 9 candidates listed in WHO

[16] will subsequently be confirmed to confer AR. However, the estimate of AR 'spread' by Tun et al. [1] when using the g440 metric, namely with all 24 mutant alleles presented with codon number greater than 440, still exceeds this upper bound. Further, it includes an additional 10 codons never included in the WHO 2018 list which was published 3 years later. In simple terms this conspicuously exposes the extent of the overestimation of AR prevalence made by Tun et al. [1] in Myanmar's case at the time of that publication.

2.3 Estimation of AR Spread

In estimating 'spread' of AR, it is critical to define exactly what is meant by 'spread'. Woodrow and White [12] allude to this by differentiating between independent 'de novo' geographic emergences of AR [20] in the sense of a 'soft sweep' of competing mutants arising and 'spread' as a 'hard sweep' in which with time, many of the soft sweep mutants decline to a few in particular. In Tun et al. [1], the usage of the word 'spread' of AR also comes with a dynamic innuendo of *spreading spatially* in time (also pointed out by Plowe and Ringwald (2015)), though this obviously cannot be supported as the data are effectively limited to a snapshot and therefore, unlike a disease time series [21], lack a temporal component.

In the current paper, I use the term 'spread' of AR in the spatial sense and distinguish this from 'spread' of AR in the population sense. In the former sense, spread is determined by a spatial measure, most fundamentally as the number of sampled sites where mutant alleles were found, which I refer to as spatial sites coverage. In the latter sense, spread is determined by the frequency of mutant alleles found in the sampled individuals from the study population.

Spatial sites coverage provides a crude summary statistic for assessing the spread of AR in terms of the proportion of sampled sites where cases of AR (by a chosen metric) were found. However, such an approach takes no account of the number of individuals sampled, other than that one or more were found presenting with an AR mutant allele at each site. Thus, if only a few individuals with AR mutant alleles were found but were located over several closely located sites, AR spread would receive a higher estimate than if many individuals were found at a few but widely dispersed sites.

On the other hand, population spread as the summary statistic for assessing spread of AR, namely as the proportion of sampled individuals where cases of AR (by a chosen metric) were found, could also be a crude estimate for AR spread because this approach takes no account of spatial information. Population spread accuracy in determining geographic prevalence is dependent only on whatever spatial diversity is (unwittingly) inherent, but this is not explicitly recorded in the configuration of site sampling locations.

When contrasted with both the above crude metrics of spread, a geostatistical model can enable a more sophisticated estimate of spread of AR to be derived by taking into account both the number of cases of AR (whatever the chosen metric) *and* the spatial site sampling locations, together with number of individuals sampled at each study site. This is achieved by spatial interpolation across the geographic domain at points where no sampling occurred, based on data, statistical modelling assumptions and knowledge. In addition, geostatistical maps readily enable a visualisation of the spatial extent of spread of AR to be compared using different metrics of interest for the given data. In this paper, I determine geostatistical maps of AR prevalence in Myanmar through the widely used Bayesian hierarchical model approach [22]. The models incorporate either the commonly used Poisson [23] or binomial [24] underlying distributional assumptions together with a Besag-York-Mollie (BYM) specification [25] and were evaluated using the R-INLA software [26,27] with details given in Appendix 1.

3. RESULTS

Fig. 2 compares the distribution of AR spread obtained by the two definitions of population proportion and spatial sites coverage in percentage, using the g440 AR metric of Tun et al. [1]. A comparison of the bar plot for spread in the spatial sites coverage sense (Fig. 2B) with that of spread in the population sense (Fig. 2A) shows that the estimate of AR spread is more accentuated when evaluated by spatial sites coverage.

Fig. 3 shows geostatistical maps of estimated AR prevalence in Myanmar obtained with the g440 metric and Tun et al. [1] data, generated by R-INLA software [26] with a BYM specification [28] and either a Poisson or binomial underlying distribution. Results for the

Poisson model are shown in the top row, with Fig. 3A showing the map of estimated AR prevalence and Fig. 3B showing the associated 'uncertainty' map. The results for the binomial model are shown in the bottom row, with Fig. 3C showing the AR prevalence map and Fig. 3D depicting the uncertainty map. The maps in Fig. 3(A and C) are strongly reminiscent, as would be expected, of those maps generated by the geostatistical Bayesian models used for estimating AR prevalence in Tun et al. [1].

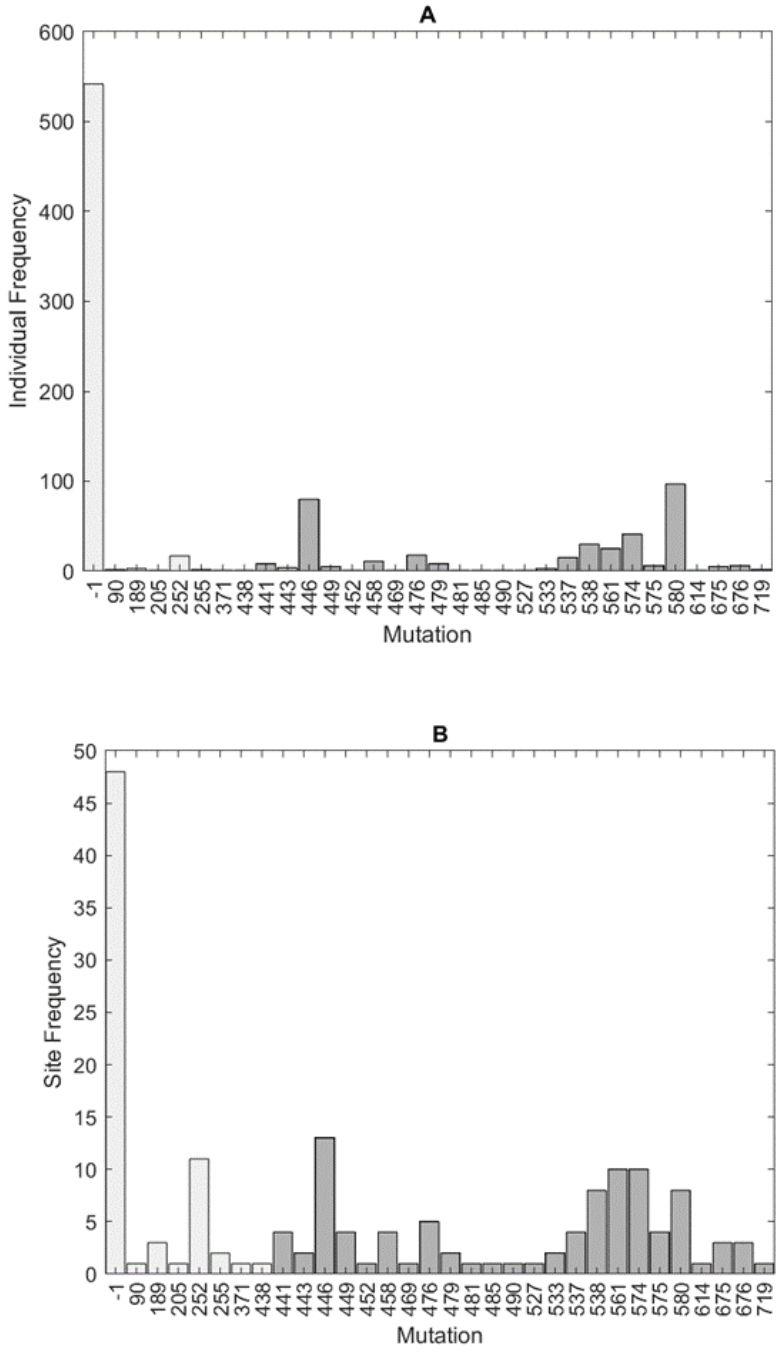

Fig. 2. Bar plots showing the codon number (with prefix and suffix letters omitted) frequencies of K13 mutant alleles as presented in the Tun et al. [1] data: (A) by number of individuals (*n*=940) and (B) by number of sites (*n*=54). The shaded bars indicate those codon numbers included in the g440 metric (those codon numbers > 440) which was used in the estimation of artemisinin resistance (AR) 'spread' by Tun et al. [1]. The -1 denotes the wild-type.

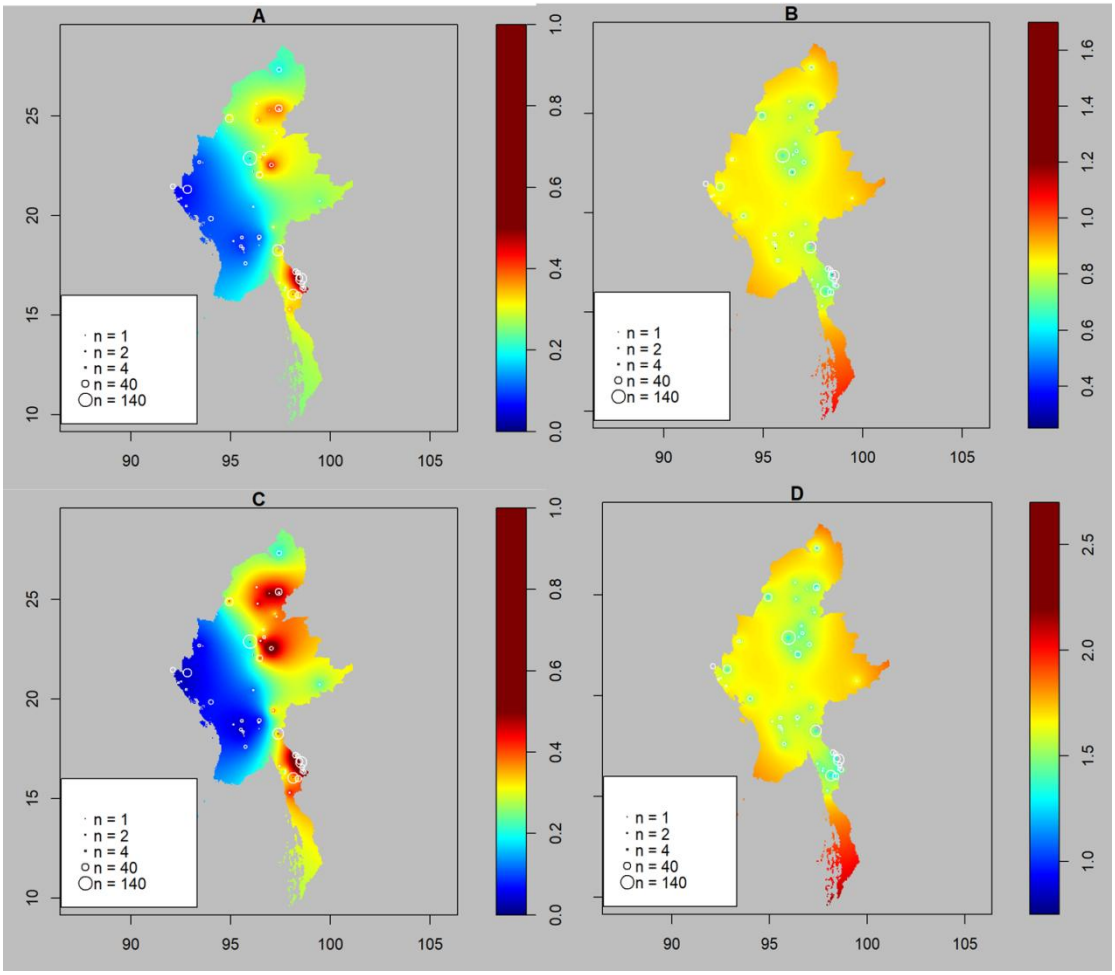

Fig. 3. Geostatistical maps of artemisinin resistance (AR) 'spread' in Myanmar generated by R-INLA with the BYM model specification using the g440 metric of Tun et al. [1] and data presented for mutant allele codons; with an underlying Poisson distribution (A) prevalence and (B) associated uncertainty; with an underlying binomial distribution (C) prevalence and (D) associated uncertainty. The colour scale in (A) and (C) ranges from dark blue (0%) to dark red (>=50%) as was scaled in Tun et al. [1]. Site sample sizes are superimposed at site locations as centred circles scaled by area in the corresponding legend box (bottom left of each frame).

A comparison of estimated AR prevalence in the Fig. 3 maps, obtained by using the g440 metric, was made with estimated AR prevalence by each of the four Metrics based on WHO data. The respective R-INLA maps as here generated, are shown in Fig. 4 for Metric 1 and Metric 2 based on the WHO [15] list of codons and in Fig. 5 for Metric 3 and Metric 4, based on the WHO [16] list.

In Fig. 4A for the Poisson model and Fig. 4C for the binomial model, where the Metric 1 consists of only the sole codon C580Y confirmed to confer AR by the WHO as at 2015,there is minimal estimated spread of AR, as represented by a tiny zone located in a south eastern location near the Kayin border with Thailand. These maps contrast strongly with the maps generated by each model shown respectively in Fig. 4B and Fig. 4D, where the confirmed *and* candidate codons in Metric 2 (9 in total) listed by the WHO as at 2015 are included. The latter maps show a wider regional estimated prevalence of AR in the eastern half of the country together with two clearly defined additional hotspots in the north at Kachin (driven by codon F446I) and immediately below that in a more central location (driven by codon P574L).

Similarly, comparisons are made in Fig. 5 for Metric 3 and Metric 4, based on the more recently confirmed and candidate mutant allele

codons published in WHO [16]. Here, the codons that were included into the AR metric are the confirmed codons of Metric 3, resulting in the R-INLA maps shown in Figs. 5A and 5C respectively for the Poisson or binomial models, or the confirmed *and* candidate codons of Metric 4 as respectively shown in Figs. 5B and 5D.

Again, the disparity between estimated prevalence of AR by Metric 3 in the geostatistical maps, as shown in Fig. 5 (A and C) when compared with those obtained by the g440 metric as shown in Fig. 3(A and C) is readily apparent.

In the former maps with Metric 3, there are only two miniscule hotspots that are indicated by red/yellow locations, consistent with those of Metric 2. One of these is located in the northern side of the country in Kachin while the other is at a south-eastern location near the Kyin border of with Thailand. However, in the latter maps of Fig. 3(A and C) with the g440 metric, these hotspots are completely subsumed within a much larger red/yellow zone, which extends along the entire eastern border region of the country on the right side of the map. In addition, there is now a large hotspot, immediately below Kachin, contained within the central region of this zone.

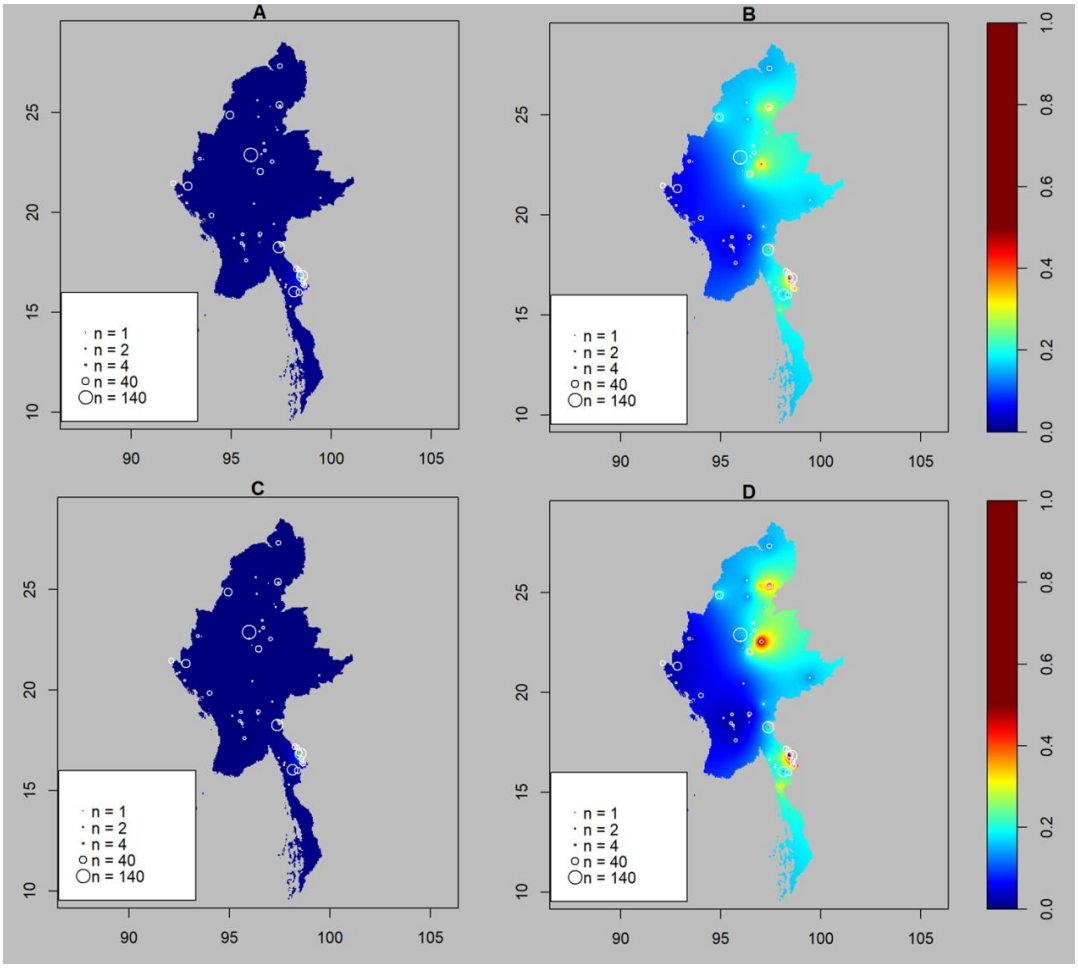

Fig. 4. Geostatistical maps of estimated AR prevalence in Myanmar generated by R-INLA with the BYM model specification using Metric 1 or Metric 2 as defined in Table 1, respectively of either K13 mutant allele *confirmed* or *confirmed and candidate* codons to confer artemisinin resistance (AR) based on the WHO [15] list, as presented in the Tun et al. [1] data. Respective maps are shown for an underlying Poisson distribution in (A) with Metric 1 and (B) with Metric 2; or for an underlying binomial distribution in (C) with Metric 1 and (D) with Metric 2. The colour scale in all the maps ranges from dark blue (0%) to dark red (>=50%) as was scaled in.Tun et al. [1]. Site sample sizes are superimposed at site locations as centred circles scaled by area in the corresponding legend box (bottom left of each frame).

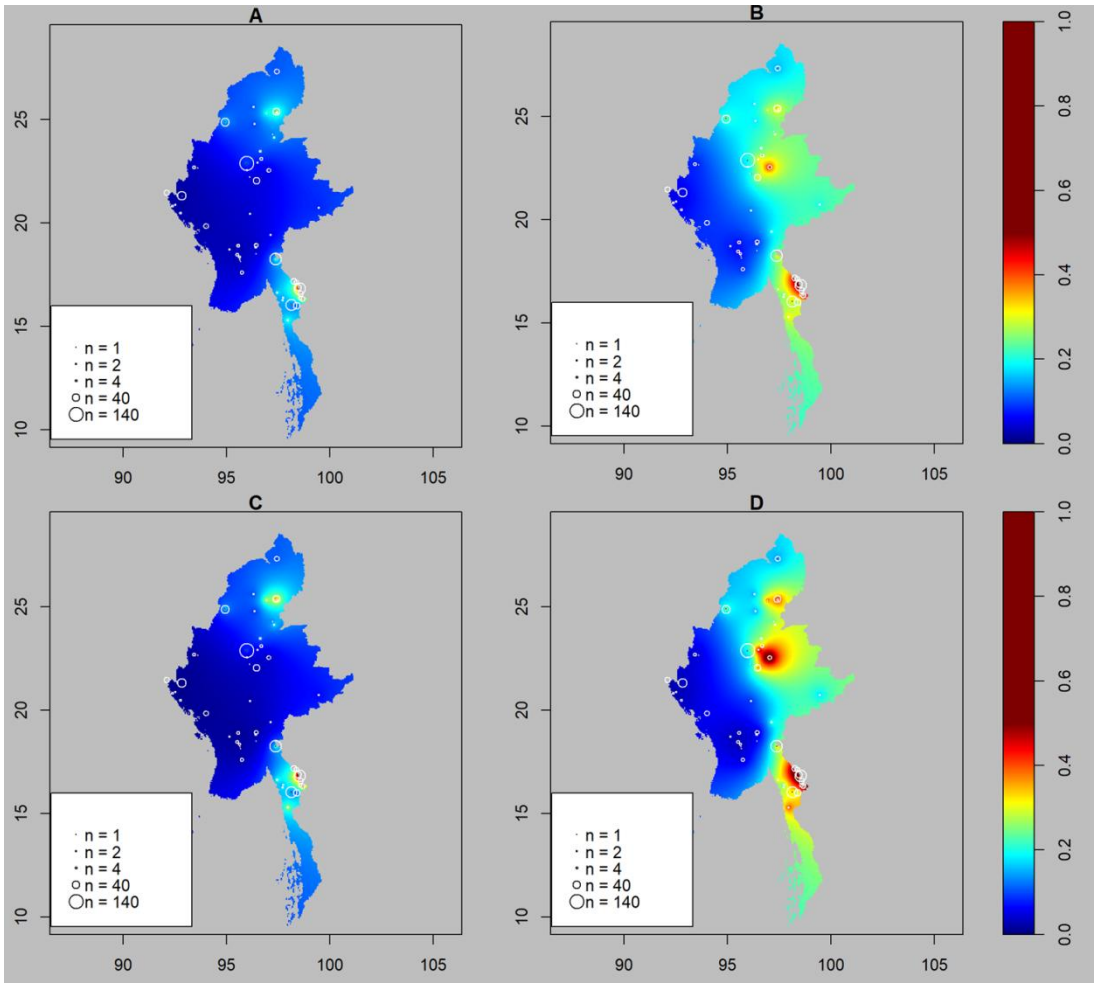

Fig. 5. Geostatistical maps of estimated AR prevalence in Myanmar generated by R-INLA with the BYM model specification using Metric 3 or Metric 4 as defined in Table 1, respectively of either K13 mutant allele *confirmed* or *confirmed and candidate* codons to confer artemisinin resistance (AR) based on the WHO [16] list, as presented in the Tun et al. [1] data. Respective maps are shown for an underlying Poisson distribution in (A) with Metric 3 and (B) with Metric 4, or for an underlying binomial distribution in (C) with Metric 3 and (D) with Metric 4. The colour scale in all the maps ranges from dark blue (0%) to dark red (>=50%) as scaled in Tun et al. [1]. Site sample sizes are superimposed at site locations as centred circles scaled by area in the corresponding legend box (bottom left of each frame).

A parallel comparison was also obtained in terms of mutant allele codon frequency distributions for either population proportions or spatial sites coverage, of the four Metrics based on the WHO [15] and WHO [16] data. These are shown as bar plots in Figs. 6 and 7 and enable a direct comparison to be made with those obtained for the g440 metric shown in Fig. 2. Fig. 7(A and C) also reveals that the estimated prevalence of AR by the benchmark Metric 3 is driven by just 5 codons (namely F446I, N458Y, M476I, R561H, C580Y) out of the 24 in total incorporated into the g440 metric used by Tun et al. [1].

Table 2 compares all the summary statistics for the g440 metric of Tun et al. [1] with those of the four WHO-based Metrics that were used for assessing the spread of AR either by population proportion, spatial site coverage or R-INLA geostatistical map. These statistics demonstrate that by using the g440 metric, consistent overestimation of AR prevalence occurs when compared to all four of the WHO- based metrics.

In the light of the Metric 3 benchmark, Metric 1 produces a clear underestimate of the prevalence of AR. This implies that the WHO perception of AR prevalence in Myanmar in

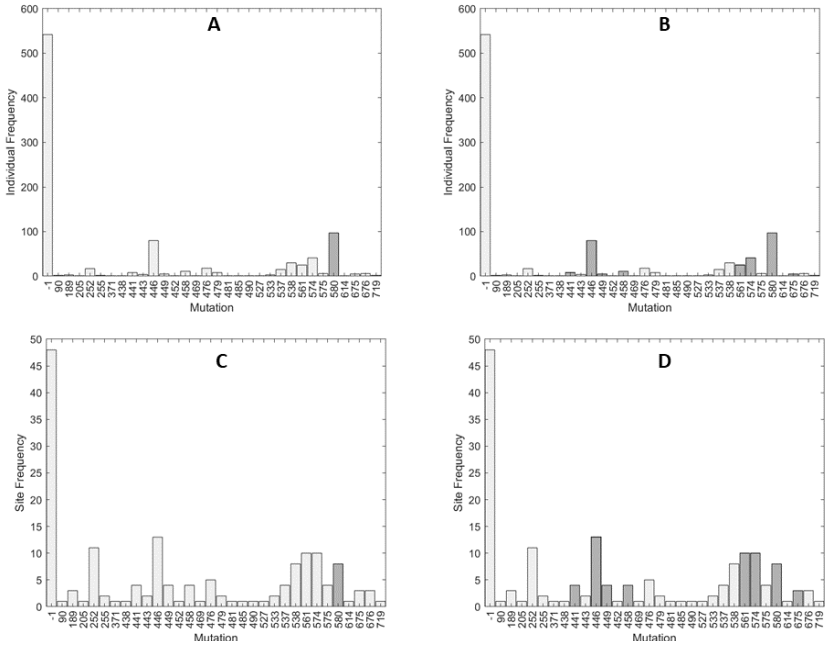

Fig. 6. Bar plots showing codon number (with prefix and suffix letters omitted) frequencies of K13 mutant alleles presented in the Tun et al. [1] data, as either *confirmed* (Metric 1) or *confirmed and candidate* codons (Metric 2) to confer artemisinin resistance (AR), based on the WHO [15] published list. The -1 denotes the wild-type. The shaded bars indicate frequencies recorded for individuals (*n*=940) in (A) by Metric 1 and (B) by Metric 2, or number of sites (*n*=54) in (C) by Metric 1 and (D) by Metric 2.

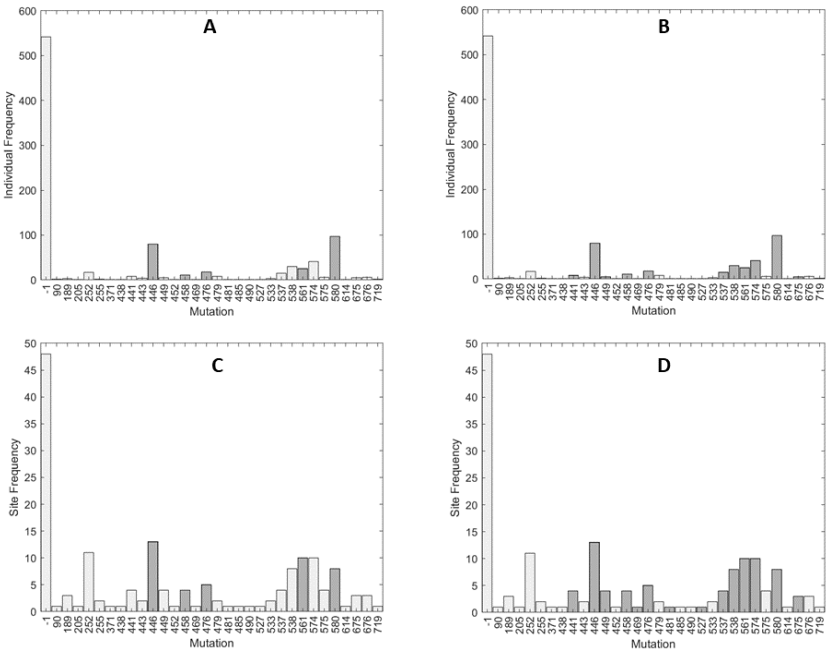

Fig. 7. Bar plots showing codon number (with prefix and suffix letters omitted) frequencies of K13 mutant alleles presented in the Tun et al. [1] data, as either *confirmed* (Metric 3) or *confirmed and candidate* codons (Metric 4) to confer artemisinin resistance (AR), based on the WHO [16] published list. The -1 denotes the wild-type. The shaded bars indicate frequencies recorded for individuals (*n*=940) in (A) by Metric 3 and (B) by Metric 4, or number of sites (*n*=54) in (C) by Metric 3 and (D) by Metric 4.

Table 2. Measures of 'spread' of artemisinin resistance (AR) estimated by the g440 metric of Tun et al. [1] and compared with the four Metrics defined in Table 1 of this paper. Metric 1 and Metric 2 are respectively defined as the K13 mutant allele *confirmed codons* or *confirmed and candidate codons* to confer AR in the WHO [15] list; Metric 3 and Metric 4 are respectively defined as the K13 mutant allele *confirmed codons* or *confirmed and candidate codons* to confer AR in the WHO [16] list. The values are shown in percentages to 2 significant figures and evaluated by using the 3 different estimation approaches of: (top panel) mean prevalence in the geostatistical map generated by R-INLA with the BYM model specification with either a Poisson or binomial underlying distribution; (middle panel) proportion of sampled population; (bottom panel) proportion of sampled sites sampled.

Summary statistic of AR spread	g440	Metric 1	Metric 2	Metric 3	Metric 4
Geostatistical map					
Poisson mean prevalence (%)	22	1.0	15	8.0	18
Binomial mean prevalence (%)	24	0.0	14	7.0	18
Population					
Population proportion (%)	39	10	29	25	36
Number of individuals (n=940)	*371*	*97*	*272*	*231*	*338*
Sites					
Sites proportion (%)	57	15	50	43	52
Number of sites (n=54)	*31*	*8*	*27*	*23*	*28*

2015, based on the codons then known to confer AR (only codon C580Y), was a clear underestimation. By the same benchmark of Metric 3, if all the candidate codons in the WHO [15] list are included to give Metric 2, an overestimation could then be produced. The overestimation could be increased by extending the Metric 3 to Metric 4 through inclusion of all the candidate codons in the WHO [16] list. However, this overestimation is still well below that produced by the g440 metric, as can be seen by a direct comparison with any of the respective summary statistics in Table 2.

Finally, a comparison of the mean estimated prevalence in Table 2, obtained with the R-INLA geostatistical maps with either of the underlying distributions (Poisson or binomial), re-enforces the point again. The mean prevalence of AR estimated by the g440 metric (22% or 24%) and by the benchmark Metric 3 (8% or 7%) differ by an overestimation factor of the order of 3. This margin is lower when a comparison is made with Metric 4 through the additional inclusion of all the candidate codons published by the WHO in 2018 (18% or 18%), however the overestimation factor is then still around one third higher by the g440 metric.

4. DISCUSSION

The Tun et al. [1] assessment of AR 'spread' in Myanmar differs radically from the AR prevalence estimated in this paper, based on WHO [15] data of mutant allele codons associated with AR. The later perspective also provided here and based on the updated WHO [16] data, although achieving a higher estimation of AR prevalence, also gives a prevalence level which is far below that estimated by Tun et al. [1].

If the choice of AR metric is restricted to mutant alleles as *confirmed to confer* AR in the WHO [16] list by the benchmark Metric 3, only two small localised hot spots of artemisinin resistance at disparate locations are identified in the south and north of Myanmar. It is impossible to view this map as 'spread' of AR as purveyed by Tun et al. [1]. Even by including all the known *candidate* mutant alleles in WHO [16] defined by Metric 4, the degree and range of contiguity in the estimated prevalence map remains far below that of the extensive geographic coverage when conveyed by the g440 metric.

The R-INLA geostatistical maps of Figs. 3, 4 and 5 of this paper strongly demonstrate the degree of disparity between estimated prevalence of AR in Myanmar by the g440 metric employed by Tun et al. [1] with that of metrics based on the WHO [15] and [16] published data. These maps demonstrate that the inclusion (or not) of *candidate* codons listed in 2015 and 2018 by the WHO has a profound influence on assessment of AR spread. They also convey a wide range for the estimated AR prevalence but, which broadly, increases in spatial coverage as the number of

mutant codons included into the AR metric are increased. This can be seen to be more pronounced in 2018, with the inclusion of more candidate codons to confer AR in the larger WHO list of 2018, by a direct comparison of all the respective maps shown in Figs. 4ABCD with those of Figs. 5ABCD.

In the light of increasing scientific knowledge on genetic markers, the WHO [15,16] data lists of confirmed and candidate mutant allele codons conferring AR may not have been necessarily definitive. Indeed, the efficacy of the role of the WHO in tackling global health matters has often been unclear and viewed with scepticism, as was re-iterated by the recent failure of many countries to heed warnings of the covid pandemic issued by the WHO in January 2020 (Maxmen 2021). However, the WHO [16] data are still the most current officially published data on codons known to either confer or to be candidates associated with conferring AR. The analysis presented in this paper shows that by asserting all codons above codon number 440 in the propeller region of the K13 genetic marker confer artemisinin resistance, as was done by Tun et al. [1], necessarily leads to an unsupportable misrepresentation of 'spread' of AR in Myanmar. Some leading authors have warned that this controversial pursuit of 'AR spread' may deflect the focus away from other key research issues such as partner-drug efficacy when used in artemisinin combination therapies (ACTs) or the importance of initial parasite densities in tackling malaria endemicity [9,10].

The current analysis shows that AR prevalence estimates in Myanmar based on metrics derived from WHO [15] and WHO [16] published data followed a logical progression. These estimates are readily supportable by geostatistical maps, which were produced from either confirmed or candidate codons then known to confer AR as listed. In addition, the WHO data sets can provide clear benchmarks to calibrate the importance of ongoing future progress of K13 mutant allele codon identification of AR.

5. CONCLUSION

While it is prudent to adopt a precautionary approach by evaluating worst case scenarios for the spread of AR, it is necessary also that the robustness of such assertions is meticulously examined to ensure that they are scientifically rigorous. This principle was notably absent in the estimation made with the g440 metric of 'spread' of AR in Myanmar by Tun et al. [1].

The danger of 'crying wolf' [8] is of also invoking 'once bitten, twice shy'. That will mean estimations of true emerging artemisinin resistance, wherever they might actually occur, are not given the attention they deserve in future research work.

CONSENT AND ETHICAL APPROVAL

It is not applicable.

ACKNOWLEDGEMENTS

I thank Dr. Alastor M. Coleby and the four anonymous reviewers for their suggestions and valuable remarks which improved the original manuscript.

COMPETING INTERESTS

Author has declared that no competing interests exist.

REFERENCES

1. Tun KM, Imwong M, Lwin KM, Win Aa, Hlaing TM, Hlaing T, Lin K, Kyaw MP, Plewes K, et al. Spread of artemisinin-resistant Plasmodium falciparum in Myanmar: a cross-sectional survey of the K13 molecular marker. The Lancet Infectious Diseases. 2015;21–26. DOI:https://doi.org/10.1016/S1473-3099(15)70032-0
2. Bwire GM, Ngasala B, Mikomangwa WP, Kilonzi M, Kamuhabwa AAR. Detection of mutations associated with artemisinin resistance at k13-propeller gene and a near complete return of chloroquine susceptible falciparum malaria in Southeast of Tanzania. Scientific Reports. 2020;10(1):1–7. DOI:https://doi.org/10.1038/s41598-020-60549-7
3. Edwards HM, Dixon R, de Beyl CZ, Celhay O, Rahman M, Oo MM, Lwin T, Lin Z, San T, et al. Prevalence and seroprevalence of plasmodium infection in myanmar reveals highly heterogeneous transmission and a large hidden reservoir of infection. PLoS ONE.2021;16(6 June):1–20. DOI:https://doi.org/10.1371/journal.pone.0252957

4. Grist EPM, Flegg JA, Humphreys G, Mas IS, Anderson TJC, Ashley EA, et al. Optimal health and disease management using spatial uncertainty: A geographic characterization of emergent artemisinin-resistant *Plasmodium falciparum* distributions in Southeast Asia. International Journal of Health Geographics. 2016;15(1):1–10. DOI:https://doi.org/10.1186/s12942-016-0064-6
5. Ariey F, Witkowski B, Amaratunga C, Beghain J, Langlois AC, Khim N, Kim S, Duru V, et al. A molecular marker of artemisinin-resistant Plasmodium falciparum malaria. Nature.2014;505(7481):50–55. DOI:https://doi.org/10.1038/nature12876
6. Zaw MT, Emran NA, Lin Z. Updates on k13 mutant alleles for artemisinin resistance in Plasmodium falciparum. Journal of Microbiology, Immunology and Infection. 2018;51(2):159–165. DOI:https://doi.org/10.1016/j.jmii.2017.06.009
7. Chookajorn T. How to combat emerging artemisinin resistance: Lessons from "The Three Little Pigs." PLoS Pathogens. 2018;14(4):4–11. DOI:https://doi.org/10.1371/journal.ppat.1006923
8. Meshnick S. Perspective: Artemisinin-resistant malaria and the wolf. American Journal of Tropical Medicine and Hygiene. 2012;87(5):783–784. DOI:https://doi.org/10.4269/ajtmh.2012.12-0388
9. Ferreira PE, Culleton R, Gil JP, Meshnick SR. Artemisinin resistance in *Plasmodium falciparum*: What is it really? Trends in Parasitology. 2013;29(7):318–320. DOI:https://doi.org/10.1016/j.pt.2013.05.002
10. Krishna S, Kremsner PG. rtemisinin resistance needs to be defined rigorously to be understood: Response to dondorp and ringwald. Trends in Parasitology. 2013;A29(8):361–362. DOI:https://doi.org/10.1016/j.pt.2013.05.006
11. Abubakar UF, Adam R, Mukhtar MM, Muhammad A, Yahuza AA, Ibrahim SS. Identification of Mutations in antimalarial resistance gene Kelch13 from *Plasmodium falciparum* isolates in Kano, Nigeria. Tropical Medicine and Infectious Disease. 2020;5(2). DOI:https://doi.org/10.3390/tropicalmed5020085
12. Woodrow CJ, White NJ. The clinical impact of artemisinin resistance in Southeast Asia and the potential for future spread. FEMS Microbiology Reviews. 2017;41(1):34–48. DOI:https://doi.org/10.1093/femsre/fuw037
13. Mok S, Stokes BH, Gnädig NF, Ross LS, Yeo T, Amaratunga C, Allman E, Solyakov L, Bottrill AR, et al. Artemisinin-resistant K13 mutations rewire *Plasmodium falciparum*'s intra-erythrocytic metabolic program to enhance survival. Nature Communications. 2021;12(1):1–15. DOI:https://doi.org/10.1038/s41467-020-20805-w
14. Siddiqui FA, Liang X, Cui L. *Plasmodium falciparum* resistance to ACTs: Emergence, mechanisms, and outlook. International Journal for Parasitology: Drugs and Drug Resistance. 2021; 16(January):102–118. DOI:https://doi.org/10.1016/j.ijpddr.2021.05.007
15. World Health Organization. Status report on artemisinin and ACT resistance, September 2015. World Health Organization; 2015. Available:https://apps.who.int/iris/handle/10665/338493
16. World Health Organization. Artemisinin resistance and artemisinin-based combination therapy efficacy: status report, August 2018.World Health Organization;2018. Available:https://apps.who.int/iris/handle/10665/274362. License: CC BY-NC-SA 3.0 IGO
17. Ménard, D, Khim, N, Beghain, J, Adegnika, A. A, Shafiul-Alam, M, Amodu, O, Rahim-Awab G, et al. A Worldwide Map of *Plasmodium falciparum* K13-Propeller polymorphisms. New England Journal of Medicine. 2016;374(25):2453–2464. DOI:https://doi.org/10.1056/nejmoa1513137
18. Yobi DM, Kayiba NK, Mvumbi DM, Boreux R, Bontems S, Kabututu PZ, et al. The lack of K13-propeller mutations associated with artemisinin resistance in *Plasmodium falciparum* in Democratic Republic of Congo (DRC). PLoS ONE. 2020;15(8 August 2020):1–9. DOI:https://doi.org/10.1371/journal.pone.0237791
19. Fairhurst RM. Understanding artemisinin-resistant malaria. Current Opinion in

Infectious Diseases. 2015;28(5):417–425. DOI:https://doi.org/10.1097/qco.0000000000000199

20. Takala-Harrison S, Jacob CG, Arze C, Cummings MP, Silva JC, Dondorp AM, et al. Independent emergence of artemisinin resistance mutations among Plasmodium falciparum in Southeast Asia. The Journal of Infectious Diseases. 2015;211(5):670–679. DOI:https://doi.org/10.1093/infdis/jiu491
21. Kaestli M, Grist EPM, Ward L, Hill A, Mayo M, Currie BJ. The association of melioidosis with climatic factors in Darwin, Australia: A 23-year time-series analysis. Journal of Infection.2016;72(6):687–697. DOI:https://doi.org/10.1016/j.jinf.2016.02.015
22. Lawson AB. Bayesian disease mapping: Hierarchical modeling in spatial epidemiology. Chapman and Hall/CRC; 2008. DOI:https://doi.org/10.1111/j.1467-985x.2010.00681_11.x
23. Walker L, Gotway C. Applied spatial statistics for public health, New York, Wiley; 2004.
24. Morgan O, Vreiheid M, Dolk H. risk of low birth weight near eurohazcon hazardous waste landfilll sites in England. Archives of Environmental Health. 2004;59:149-151.
25. Samat NA, Mey LW. Malaria disease mapping in Malaysia based on Besag-York-Mollie (BYM) Model. Journal of Physics: Conference Series. 2017;890(1). DOI:https://doi.org/10.1088/1742-6596/890/1/012167
26. Lindgren F, Rue H. Bayesian spatial modelling with R-INLA. Journal of Statistical Software.2015;63(19):1–25. DOI:https://doi.org/10.18637/jss.v063.i19
27. Rue H, Martino S, Chopin N. Approximate Bayesian inference for latent Gaussian models by using integrated nested Laplace approximations. Journal of the Royal Statistical Society: Series B (Statistical Methodology). 2009;71(2):319–392. DOI:https://doi.org/10.1111/j.1467-9868.2008.00700.x
28. Besag J, York J, Mollié A. A Bayesian image restoration with two applications in spatial statistics Ann Inst Statist Math. 1991;43:1–59. Find This Article Online.43(1):1–20.

APPENDIX 1

Poisson model

The case count y_i is assumed to have a mean μ_i within each small area *i* of the gridded 5km x 5km [= 0.04159721 decimal degree square] domain covering the whole of the Myanmar map, plotted as latitude (vertical axis) against longitude (horizontal axis) in decimal degrees and to be independently distributed as

$$y_i \sim Poisson(\mu_i)$$

so the likelihood is

$$L(\boldsymbol{y}|\boldsymbol{\mu}) = \prod_{i=1}^{m} \mu_i^{y_i} \exp(-\mu_i)/y_i!$$

The usual assumption is made that data are independently distributed with expectation

$$E(y_i) = \mu_{\mathrm{i}} = \mathrm{e_i}\theta_i$$

where $\mathrm{e_i}$ is the expected rate for the *i*th area, θ_i is the relative risk for the *i*th area and $\{y_i\}$ are assumed to be conditionally independent given knowledge of $\{\theta_i\}$.

The relative risk θ_i is then modelled as a linear predictor by assuming the logarithmic link

$$log\theta_i = \eta_i$$

Binomial model

The probability of a case is assumed to be p_i and the case count y_i within each small area *i* of the gridded 5km x 5km domain [covering the whole of the Myanmar map] is assumed to be distributed independently as

$$y_i \sim bin(p_i, n_i)$$

so, the likelihood is

$$L(y_i|p_i, n_i) = \prod_{i=1}^{m} \binom{n_i}{y_i} p_i^{y_i} (1 - p_i)\,(1 - p_i)^{(n_i - y_i)}$$

and for $p_i$to be a linear predictor, a logit link is chosen so that

$$p_i = \frac{exp(\eta_i)}{1 + exp(\eta_i)}$$

The BYM model is then specified by

$$\eta_i = \alpha + \nu_i + \upsilon_i$$

where

$$\nu_i \sim Normal(0, \tau_\nu^2)$$

is the unstructured residual and

$$v_i | v_{j \neq i} \sim Normal(\overline{v_i}, \tau_i^2)$$

is the spatially structured residual modelled as an intrinsic conditional autoregressive (iCAR) structure with

$$\overline{v_i} = \frac{\sum_{j \in N(i)} v_j}{\#N(i)}$$

and

$$\tau_i^2 = \frac{\tau_v^2}{\#N(i)}$$

where $N(i)$ denotes a neighbouring area to area *i* and $\#N(i)$ denotes the number of areas which have boundaries with the *i*th one. So τ_v^2 and τ_v^2control the random effects respectively in v_i and v_i .

© 2022 Grist; This is an Open Access article distributed under the terms of the Creative Commons Attribution License (http://creativecommons.org/licenses/by/4.0), which permits unrestricted use, distribution, and reproduction in any medium, provided the original work is properly cited.

Peer-review history:
The peer review history for this paper can be accessed here:
https://www.sdiarticle5.com/review-history/89422